Biochemical and Biophysical Research Communications 456 (2015) 434–439

Contents lists available at ScienceDirect

Biochemical and Biophysical Research Communications

journal homepage: www.elsevier.com/locate/ybbrc

Parthenolide induces autophagy via the depletion of 4E-BP1

Bei Lan [a,b], Ya-Juan Wan [a], Shuang Pan [a], Yu Wang [a], Yin Yang [b], Qian-Li Leng [b], Huiyan Jia [b], Yao-hui Liu [b], Cui-Zhu Zhang [a,*], Youjia Cao [a,b,*]

[a] Key Laboratory of Microbial Functional Genomics of Ministry of Education, College of Life Sciences, Nankai University, 94 Weijin Road, Tianjin 300071, PR China
[b] State Key Laboratory of Medicinal Chemical Biology, College of Life Sciences, Nankai University, 94 Weijin Road, Tianjin 300071, PR China

ARTICLE INFO

Article history:
Received 21 November 2014
Available online 4 December 2014

Keywords:
Parthenolide
Autophagy
Apoptosis
4E-BP1
Reactive oxygen species

ABSTRACT

Parthenolide (PTL) is a sesquiterpene lactone isolated from feverfew and exhibits potent antitumor activity against various cancers. Many studies indicate that PTL treatment leads to apoptosis, however, the mechanism has not been defined. Here, we observed that cells underwent autophagy shortly after PTL treatment. Inhibition of autophagy by knocking out autophagy associated gene *atg*5 blocked PTL-induced apoptosis. Surprisingly, PTL decreased the level of translation initiation factor eIF4E binding protein 1 (4E-BP1) in correlation with autophagy. Ectopic expression or shRNA knockdown of 4E-BP1 further verified the effect of 4E-BP1 on PTL-induced autophagy. Meanwhile, PTL elevated the cellular reactive oxygen species (ROS) which located upstream of the depletion of 4E-BP1, and contributed to the consequent autophagy. This study revealed 4E-BP1 as a trigger for PTL-induced autophagy and may lead to therapeutic strategy to enhance the efficacy of anticancer drugs.

1. Introduction

Parthenolide (PTL), a 10+5 ring type sesquiterpene lactone, was first isolated from *Tanacetum parthenium* as the predominant component of feverfew [1]. It is emerging as a promising anticancer drug based on its antitumor activity by inducing cell apoptosis in various cancers, such as cholangiocarcinoma [2], and acute myeloid leukemia (AML) [3]. Accumulated evidence indicates that PTL induces apoptosis by elevation of the oxidative stress [4], disintegration of mitochondria membranes [5], and inhibition of NF-κB activity [6].

The clinical application of PTL has been suggested when combined with chemotherapeutic drugs. For example, parthenolide and sulindac cooperatively block cell growth in pancreatic carcinoma cells [7]. It seems that PTL exerts its anticancer role by increasing the sensitivity of cells to the drugs, rather by directly killing cells. In this regards, PTL mediated cellular events is to be resolved.

Autophagy is a cellular process for the degradation of cytoplasmic organelles or cytosolic components, and has been originally considered as a protective factor for cells [8]. Nowadays, it is widely accepted that autophagy plays both pro-survival and pro-death effects in cancer cells [9]. Thereby, the resolution of PTL-induced autophagy and its consequences would provide biological basis for the clinical application of PTL in cancer therapy.

In this report, we showed that PTL treatment resulted in autophagy in human promyelocytic leukemia cell line, HL-60, and human epithelial carcinoma cell line, HeLa. We found that PTL induced autophagy was closely related to the decreased level of 4E-BP1, independent of its function as regulating factor for eukaryotic initiation factor 4E (eIF4E). Withdraw of the oxidative stress significantly blocked the reduction of 4E-BP1 in PTL treated cells. This study uncovered 4E-BP1 as a trigger for autophagy in PTL treatment and may lead to new strategy to enhance the efficacy of anticancer drugs.

2. Materials and methods

2.1. Reagents and antibodies

Parthenolide (PTL) was kindly provided by Dr. Yue Chen (Nankai University, China). Annexin V apoptosis Detection Kit

Abbreviations: PTL, parthenolide; eIF4E, eukaryotic initiation factor 4E; 4E-BP1, translation initiation factor eIF4E binding protein 1; AML, acute myeloid leukemia; ER, endoplasmic reticulum; ROS, reactive oxygen species; mTOR, mammalian target of rapamycin; MEF, mouse embryonic fibroblast.

* Corresponding authors at: Rm. 224, Molecular Biology Institute, Nankai University, 94 Weijin Road, Tianjin 300071, PR China. Fax: +86 (22) 23500808 (Y. Cao).

E-mail addresses: czz912@aliyun.com (C.-Z. Zhang), caoyj@nankai.edu.cn (Y. Cao).

http://dx.doi.org/10.1016/j.bbrc.2014.11.102
0006-291X/

(559763) was purchased from BD Biosciences (San Jose, CA, USA). N-acetyl-cysteine (NAC) (S0077), MG132 (S1748) and SP600125 (S1876) were purchased from Beyotime (Jiangsu, China). Glutathione (GSH) (G0399) was purchased from Sangon Biotech (Shanghai, China). Anti-LC3 (L7543) and anti-Tubulin (T6074) antibodies were purchased from Sigma (St Louis, MO, USA). Anti-4E-BP1 (#9644), anti-JNK (#9258) and anti-phospho-JNK (Thr183/Tyr185) (#9255) antibody were obtained from Cell Signaling Technology (Danvers, MA, USA). Antibodies against p70S6K (sc-8418) and phospho-Ser411 p70S6K (sc-8416) were purchased from Santa Cruz Biotechnology (Santa Cruz, CA).

2.2. Cell culture

HL-60 cells, HeLa cells, and HEK293T cells were originally obtained from American Type Culture Collection (ATCC). HeLa cell line stably expressing GFP-LC3 was established by transfected with pGFP-LC3 plasmid and selected in 96-well plates for a single-cell clone. Wild-type mouse embryonic fibroblast (*WT* MEF) and *atg5* gene knock-out MEF (*atg5*$^{-/-}$ MEF) were kindly provided by Dr. Quan. Chen (Nankai University, China). The cells, except for HL-60, were kept in Dulbecco's modified Eagle's medium (DMEM) supplemented with 10% (v/v) fetal bovine serum (FBS) and 1% (v/v) penicillin/streptomycin (PS). The HL-60 cells were cultured in Roswell Park Memorial Institute (RPMI) 1640 medium supplemented with 10% FBS and 1% (v/v) PS.

2.3. Plasmid constructs

The coding region of 4E-BP1 was cloned from human cDNA made from HeLa cells by PCR. The PCR product was subcloned into EcoRI/BamHI site of pCDH-CMV-MCS-EF1-puro plasmid and named as pCDH-4E-BP1. 4E-BP1 mutants, T37A/T46A and Y54A/L59A, were generated by using PCR site-directed mutagenesis of 4E-BP1 sequences and cloned into pCDH-CMV-MCS-EF1-puro plasmid.

To knockdown the expression of 4E-BP1 by short hairpin RNA (shRNA), the target sequence, as described previously [10], was constructed into vector pLKO.1-TRC-puromycin and named as sh4E-BP1.

2.4. Lentivirus-based transduction

To knockdown the expression of 4E-BP1, the shRNA constructs (sh4E-BP1 and shCtrl) were transfected into 293T cells with the packaging plasmids (pVSVG, pMDLG, and pRSV-REV). At 48 h post-transfection, lentivirus pellets were harvested by centrifuged at 20,000*g* for 1.5 h at 4 °C, resuspended in fresh culture medium and incubated with HeLa cells for 24 h. The transduced cells were cultured for 4 days before selection with 1 μg/mL puromycin and the cells stably expressing sh4E-BP1 were used as indicated.

2.5. Western Blot analysis

Cells were lysed with the RIPA buffer (25 mM Tris–HCl, pH 7.4, 150 mM NaCl, 5 mM EDTA and 1% Triton X-100 (v/v), 1 mM PMSF, 1 mM NaF and 1 μg/mL leupeptin) and then boiled with 1× gel loading buffer (50 mM Tris–HCl, pH 7.2%, 2% SDS (m/v), 0.1% bromophenol blue, 5% glycerol, 100 mM β–mercaptoethanol). Samples were subjected to 15% sodium dodecyl sulfate polyacrylamide gel electrophoresis (SDS–PAGE), transferred to polyvinylidene difluoride (PVDF) membranes, and identified with indicated antibodies.

2.6. GFP-LC3 puncta analysis

HeLa cells stably expressing GFP-LC3 were treated with PTL and observed by fluorescence microscope (Axio Imager Z1; Zeiss, Oberkochen, Germany) with a 40× objective. 4 GFP-LC3 puncta per cell were defined as autophagic cells. A minimum of 100 cells under each experimental condition were counted and presented as percentage of autophagic cells.

2.7. Apoptosis assays

Wild-type and *atg5*$^{-/-}$ MEF cells were treated with PTL for 6 h respectively. Apoptosis was determined by Annexin V-FITC Apoptosis Detection Kit according to the manufacturer's instructions and analyzed by flow cytometer (FACS Calibur; Becton Dickinson, Franklin Lakes, NJ, USA). 10,000 events were collected and analyzed using Cell Quest software (Becton Dickinson).

2.8. Statistical analysis

Statistical analysis was performed using Student's *t*-test and values were considered statistically significant at $p < 0.05$. If not specified, all the quantitative data were presented as mean value ± standard deviation (S.D.) of three independent experiments ($n = 3$).

3. Results

3.1. PTL induces autophagy and facilitates apoptosis

The formation of autophagosomes was visualized in HeLa cells stably expressing GFP-LC3 in the presence of PTL as indicated (Fig. 1A) and nearly 90% of cells became autophagic cells (Fig. 1B). Since PTL is a promising drug candidate for leukemia and lymphoma [3,11], we examined the effect of PTL on human promyelocytic leukemia cell line, HL-60 (Fig. 1C and D), and other leukemia cells (data not shown). The level of LC3-II increased with the concentration of PTL, suggesting that PTL induce autophagy in a dose-dependent manner.

Many reports indicate that PTL induces apoptosis of tumor cells [2,3]. Meanwhile, autophagy has been considered to engage in a complex interplay with apoptosis [9]. Therefore, we attempted to resolve the effect of autophagy in regard to PTL-associated apoptosis. Wild-type MEF (*WT* MEF) and an autophagy-defective cell line (*atg5*$^{-/-}$ MEF), were incubated in the absence or the presence of PTL, and apoptotic cells were stained by fluorescence-conjugated Annexin-V (AV). FACS analysis (Fig. 1E and F) indicated that the spontaneous AV^{+} cells were about ~8% in wild type and *atg5*$^{-/-}$ cells (Fig. 1E, upper panels, and 1F, open bars). Upon PTL treatment, 93.1% of wild-type MEF cells underwent apoptosis, whereas only 33.9% of *atg5*$^{-/-}$ MEF cells were AV^{+} (Fig. 1E, lower panels, and F, close bars), indicating that PTL-induced apoptosis requires a functional machinery of autophagy.

3.2. PTL decreases the expression of 4E-BP1 in correlation with autophagy

It has been widely recognized that mTOR is a central protein kinase in the regulation of autophagy [8]. As mTOR kinase activity can be inferred by the phosphorylation state of its two substrates, p70S6K and 4E-BP1 [12], we investigated the effect of PTL on the phosphorylation of these mTOR substrates. As shown in Fig. 2A and B, PTL neither altered the phosphorylation (p-Ser411) nor the expression of p70S6K. Surprisingly, the phosphorylation and expression of 4E-BP1 were dramatically decreased (Fig. 2A, the third and fourth rows). We further confirmed that PTL reduced 4E-BP1 level in a dose dependent manner (the plotted panels) in both HL-60 (Fig. 2C) and HeLa cells (Fig. 2D). Intriguingly, the increase of LC3-II correlated well with the decrease of 4E-BP1

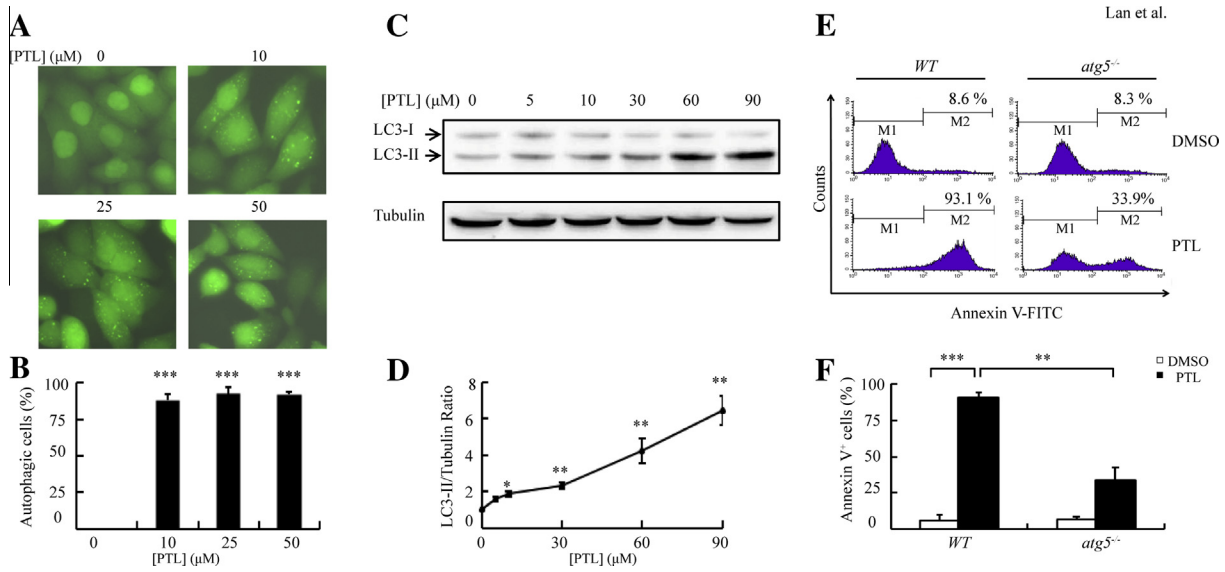

Fig. 1. PTL-induced autophagy and apoptosis. (A) HeLa cells stably expressing GFP-LC3 were treated with indicated concentrations of PTL, and visualized by fluorescence microscopy. The autophagic cells were counted as described in Section 2, and were presented as the mean values ± S.D. of percentage in bar graph (B) (error bar represents S.D., and the following is the same). $^{***}p < 0.001$, $n = 3$. (C) HL-60 cell were treated with indicated concentrations of PTL for 1.5 h. LC3 and tubulin (loading control) were resolved by Western Blot analysis. The intensities of LC3-II bands were quantified using Image J analysis software and corrected by the band intensity of tubulin. The ratio of LC3-II to tubulin was normalized to that of control sample (PTL = 0) and plotted as vertical axis of the curve graph (D). Data were shown as the mean values ± S.D. $^{*}p < 0.05$; $^{**}p < 0.01$, $n = 3$. (E) *WT* MEF (left column) and *atg5*$^{-/-}$ MEF (right column) were incubated with DMSO (upper panel) or 30 μM PTL (bottom panel) for 6 h. The induction of apoptosis was determined by flow cytometric analysis of Annexin V-FITC. The M1 and M2 gates AV^{-} and AV^{+} populations, respectively. The percentages of AV^{+} cells were presented in (F) with the mean values ± S.D. $^{**}p < 0.01$; $^{***}p < 0.001$, $n = 3$.

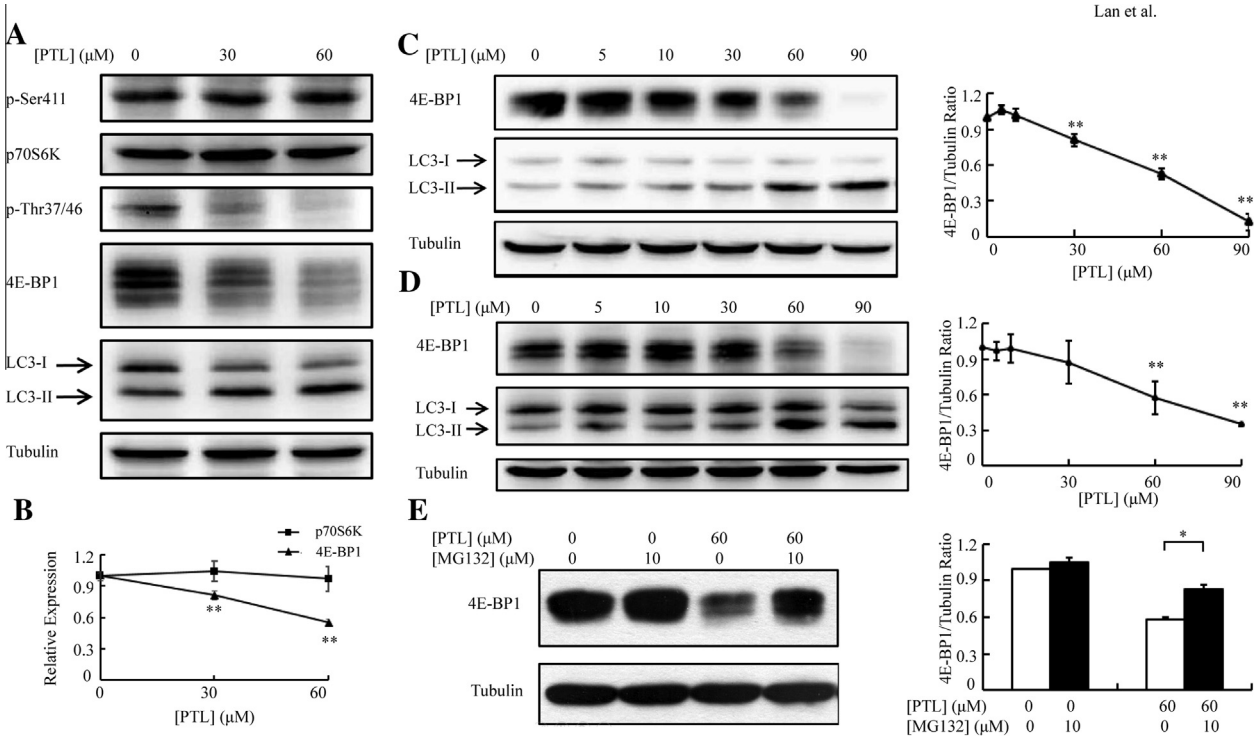

Fig. 2. Correlation of PTL-induced autophagy and 4E-BP1. (A) HL-60 cells were incubated with PTL for 1.5 h and cell lysates were subjected to Western Blot analyses, using antibodies against the phosphorylated forms of p70S6K (P-Ser411), 4E-BP1 (p-Thr37/46) , and the total proteins, respectively. (B) The band densities of p70S6K (square) and 4E-BP1 (triangle) were presented as ratio to tubulin. $^{**}p < 0.01$, $n = 3$. HL-60 (C) and HeLa (D) cells were treated with indicated concentrations of PTL. 4E-BP1 and LC3 were resolved by Western Blot, and quantitated by the ratio to tubulin. The normalized ratio of 4E-BP1 to tubulin was presented in side graph with the mean values ± S.D. $^{**}p < 0.01$, $n = 3$. (E) HeLa cells were treated with PTL for 1.5 h in the presence or absence of 10 μM MG132 and 4E-BP1 expression was detected by Western Blot. The bar graph indicated the band densities of 4E-BP1. $^{*}p < 0.05$, $n = 3$.

(Fig. 2C and D). These data implied a pivotal role of 4E-BP1 in PTL-induced autophagy.

Next, we wanted to investigate the mechanism of PTL-induced 4E-BP1 depletion. Because transcription and translation of 4E-BP1 was not affected by PTL (data not shown), we accessed proteasomal degradation by introducing MG132, a proteasome inhibitor, to the measure of 4E-BP1. As shown in Fig. 2E, the loss of 4E-BP1 by PTL (Fig. 2E, lane 3) was restored by the presence of MG132

(Fig. 2E, lane 4), suggesting that PTL leads to a decrease in 4E-BP1 via proteasome degradation.

3.3. PTL-induced autophagy is associated with the amount of 4E-BP1, but not with its function in translational regulation

4E-BP1 is widely recognized as a regulator of cap-dependent protein translation [13,14]. Given that PTL treatment reduced 4E-BP1 and concurrently induced autophagy, we next asked whether the amount of cellular 4E-BP1 is a determinant factor for autophagy. On one hand, knockdown of endogenous 4E-BP1 by shRNA (Fig. 3A, middle panel) increased LC3-II by ~50% (Fig. 3A and B). On the other hand, the overexpression of 4E-BP1 (Fig. 3C) reduced the PTL-induced LC3-II (Fig. 3C, lane 4 from the left) to ~50% of that in control vector (lane 2). Notably, the recombinant 4E-BP1 was also decreased upon PTL treatment (Fig. 3C, lane 4, middle panel).

4E-BP1 represses the initiation of protein translation via binding with eIF4E and the functional phosphorylation of 4E-BP1 releases its association with eIF4E [15]. Therefore, we employed two mutations of 4E-BP1: T37A/T46A, to eliminate phosphorylation at N-terminus and enhance the binding with eIF4E [16]; and Y54A/L59A, to abrogate the affinity with eIF4E [17,18]. As shown in Fig. 3C, cells baring mutations, T37A/T46A and Y54A/L59A, exhibited PTL-induced autophagy (Fig. 3C, lanes 6 and 8, upper panel) to the same extent as wild type 4E-BP1 (WT) (lane 4). As shown by the relative level of LC3-II under each transfection (Fig. 3D), PTL induced autophagy was suppressed to ~50% by the overexpression of 4E-BP1 or the mutations, regardless of their different effects on protein translation.

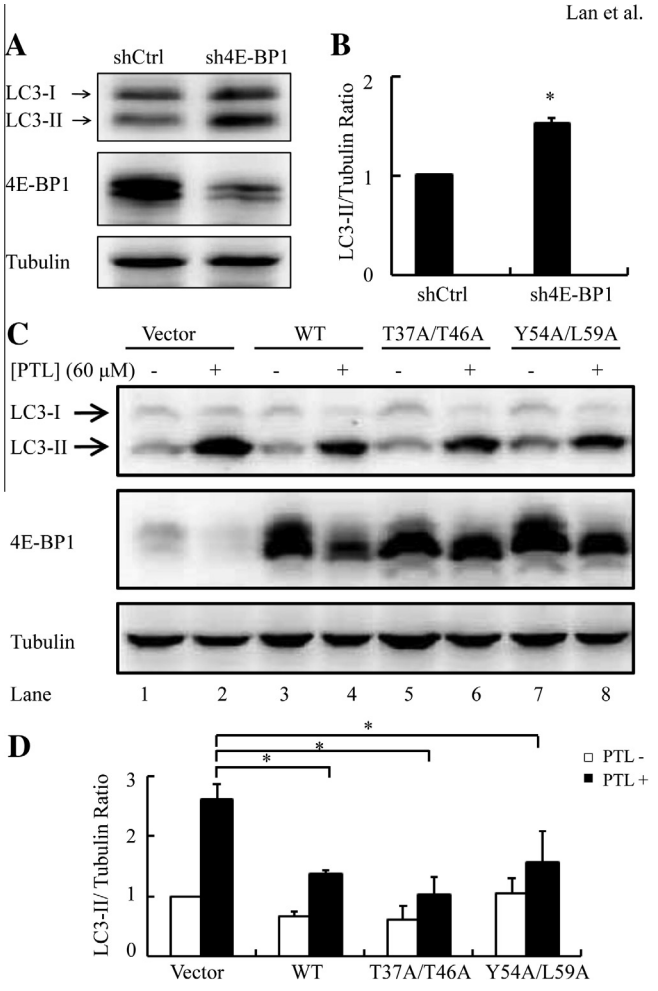

Fig. 3. Effect of 4E-BP1 on PTL-induced autophagy. (A) Transduced cells with control shRNA (shCtrl, left lane) or shRNA against 4E-BP1 (sh4E-BP1, right lane) by lentivirus were analyzed by Western Blot with indicated antibodies. (B) The band densities of LC3-II were quantitated and presented as ratio to tubulin. $^{*}p < 0.05$, $n = 3$. (C) HeLa cells transfected with control plasmid (Vector), or plasmids encoding wild-type 4E-BP1 (WT), or 4E-BP1 mutations T37A/T46A and Y54A/L59A, respectively, were treated without (−) or with (+) PTL, and subjected to Western Blot analysis. (D) The amounts of LC3-II were quantitated as described above and presented as mean ratio to tubulin ± S.D. $^{*}p < 0.05$, $n = 3$.

3.4. PTL-specific ROS mediates autophagy via 4E-BP1

PTL is known to generate oxidative stress by the depletion of glutathione (GSH) [4,19], and the involvement of ROS in autophagy is observed in the treatment of a number of chemotherapeutic agents [20]. Indeed, a significant increase in ROS was observed when cells were treated with PTL (data not shown). Is PTL-induced ROS attributes to autophagy? To answer this question, we performed GFP-LC3 puncta analysis in the presence of PTL as well as NAC, a widely recognized reagent to neutralize ROS. In comparison with control, 95% of cells underwent autophagy in the presence of PTL, whereas in the presence of NAC, the LC3 puncta were hardly observed (Fig. 4A and B). Further, elevated LC3-II induced by PTL was completely abrogated by NAC or GSH (Fig. 4C, middle panel, lanes 5, 6 and 7), confirming the participation of ROS in PTL-induced autophagy. Concurrently, as the level of 4E-BP1 was lowered dramatically by PTL (Figs. 2 and 4C, lane 5), the addition of NAC or GSH rescued 4E-BP1 to same level as the control (Fig. 4C, lanes 6, 7, and 1, respectively). Interestingly, ROS raised by hydrogen peroxide (H_2O_2) exhibited no induction of autophagy represented by LC3-II, nor effect on 4E-BP1 (Fig. 4C, lane 4). These data suggested that PTL-induced oxidative stress is required for the downregulation of 4E-BP1 which contributes to autophagy.

The oxidative stress conveys a series of cellular responses, such as the activation of MAP Kinases [21]. We aimed to explore further on how PTL-induced ROS results in 4E-BP1 depletion by examining the phosphorylation and activation of three typical MAPKs, JNK (Fig. 4D), ERK, and p38 (data not shown). As shown in Fig. 4D, elevated phosphorylation of JNK2 was seen in PTL treated cells (lane 2 from left). Unfortunately, the presence of JNK inhibitor, SP600125, failed to resume the expression of 4E-BP1 (lane 3 from left), suggesting that the depletion of 4E-BP1 by PTL, though mediates by ROS, is independent of JNK. Similar results were obtained with ERK and p38 (data not shown), and molecules involved in PTL evoked events were under investigation.

Taken together, our data emphasized the involvement of three factors along PTL-induced cell death: the PTL-induced ROS, the decrease of 4E-BP1, and autophagy (Fig. 4E). Though we cannot ruled out the contribution of PTL-induced ROS to apoptosis or autophagy bypassing 4E-BP1, our data unveiled 4E-BP1 as a key element in PTL's effect on tumor cells. This study may be of significance in diagnosis or therapeutic strategy to enhance the drug sensitivity by modulating the level of 4E-BP1 and triggering autophagy.

4. Discussion

The anticancer effect of PTL and its induction of apoptosis are studied in malignant cancers, particularly the lymphocytes disorders, such as acute myelogenous leukemia and B-chronic lymphocytic leukemia [3,11]. The molecular mechanisms behind PTL treatment is rather limited to the induction of ROS [4,19] and covalent modification of NF-κB [6]. We reported here that PTL triggered cell autophagy in several cell lines, including HL-60 (Fig. 1), Jurkat

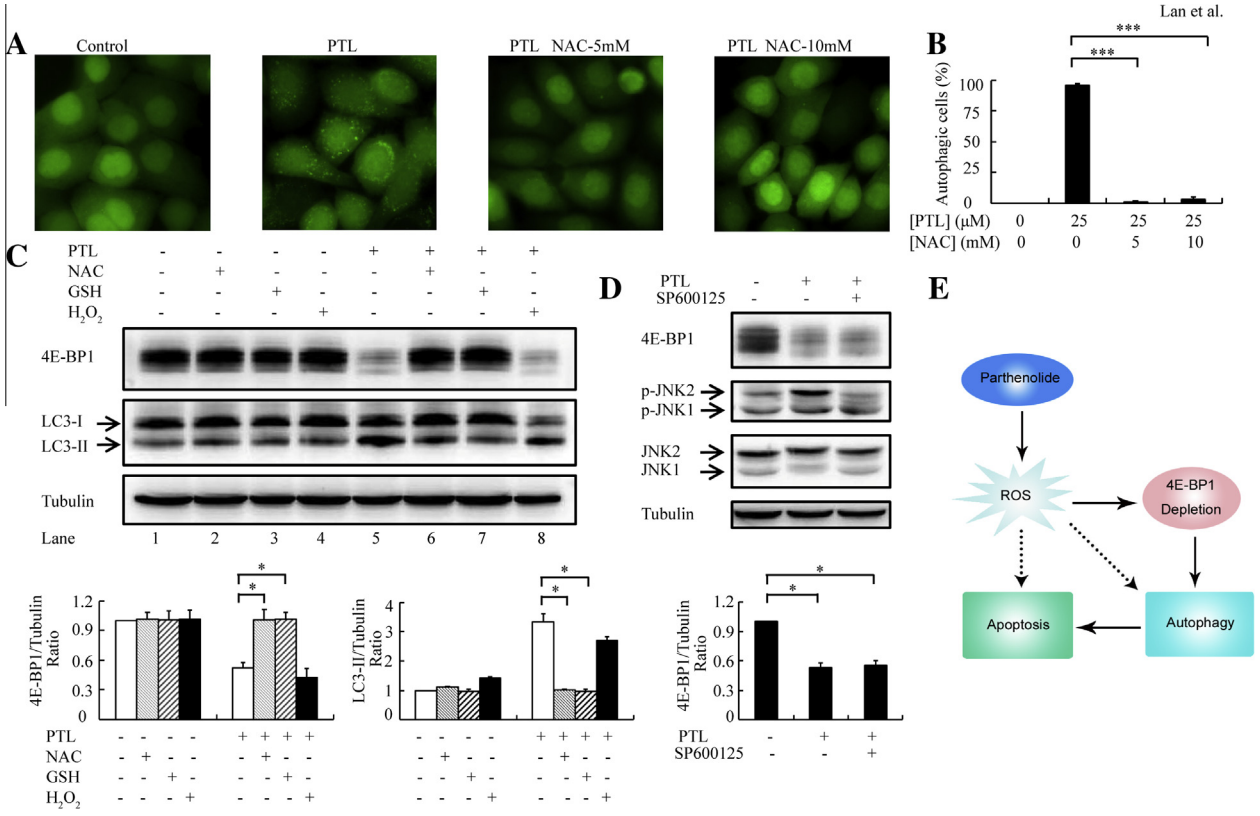

Fig. 4. Involvement of ROS and 4E-BP1 in PTL-induced autophagy. (A) GFP-LC3 puncta were observed in cells under indicated treatments by fluorescence microscopy. DMSO was used as vehicle control. (B) The bar graph indicated the mean percentages of autophagic cells ± S.D. under each condition. $^{***}p < 0.001$, $n = 3$. (C) HL-60 cells were treated with either 2.5 mM NAC/GSH or 1 mM H_2O_2 alone or in combination with 60 μM PTL for 1.5 h as indicated, and cell lysates were subjected to Western Blot. The quantitation of bands were analyzed and bar graphs presented the mean values ± S.D. $^{*}p < 0.05$, $n = 3$. (D) HL-60 cells were incubated with 60 μM PTL for 1.5 h without or with 30 μM JNK inhibitor (SP600125) as indicated on the top. 4E-BP1, activated JNK (p-JNK), and total JNK were determined by Western Blot analysis. The band densities of 4E-BP1 were presented as mean ratio to tubulin with S.D. $^{*}p < 0.05$, $n = 3$. (E) Depicted model of PTL-induced autophagy. The drug PTL mediates the generation of oxidative stress (ROS) and the depletion of 4E-BP1 in cells, which then commits to autophagy and ultimately apoptosis (solid arrows). ROS in general may promote cell apoptosis and/or autophagy independent of 4E-BP1 (the dotted line).

(data not shown), and HeLa (Fig. 1). Recently, induction of autophagy by PTL was also observed in breast cancer cells and liver cancer cell line [22–24]. Besides, two other sesquiterpene lactones, helenalin and eupalinin A, lead to autophagy of human ovarian cancer cell line (A2780) and HL-60 cells, respectively [25,26]. It is likely that sesquiterpene lactones induce cell autophagy in transition to apoptosis.

Autophagy is originally considered to be cytoprotective under several circumstances [27], and pro-apoptotic in some cellular settings. For example, platonin-induced autophagy leads to the death of human leukemia cells [28]. Our data here also suggested that the functional autophagy machinery is required for PTL-induced apoptosis using the genetically manipulated MEF cells. As autophagy and apoptosis are general cell processes, it remains to be clarified how the two processes are orchestrated.

The decrease of 4E-BP1 are observed in cells treated by several anticancer drugs, such as Bortezomib and YXM110 [29,30], in which hyperphosphorylation and proteasomal degradation of 4E-BP1 are suggested [30]. Indeed, MG132 was seen to rescue 4E-BP1 to the level similar to non-PTL sample. However the detection of 4E-BP1 phosphorylation at several sites was not conclusive, as the phosphorylated 4E-BP1 was decreased simultaneously upon PTL treatment even at lower doses. Of note, we didn't see the activation of mTOR, implying the phosphorylation and degradation of 4E-BP1 may be though alternative pathways. Other kinases may participate in the context of PTL treatment.

Given that PTL introduces oxidative stress, which in turn activates MAPKs, we attested the involvement of ROS in the downregulation of 4E-BP1 in two folds: (1) NAC and GSH abrogated PTL-induced depletion of 4E-BP1 (Fig. 4C); and (2) PTL stimulated the activation of JNK via ROS (data not shown). However, the decrease of 4E-BP1 was not rescued by the inhibitor of JNK (Fig. 4E) and other two MAPKs, ERK and p38 (data not shown). The depletion of 4E-BP1 emerged more specific for PTL as H_2O_2, though arose ROS-mediated responses, didn't affect the amount of 4E-BP1. Perhaps the regulation of 4E-BP1 responses discriminatingly to PTL-mediated oxidative stress due to the depletion of glutathione [4]. Further studies will be focused on the identification of the intermediator within PTL-induced ROS and 4E-BP1.

Nevertheless, our data proposed a strong link of autophagy as a downstream event of 4E-BP1 reduction. This notion was also supported by studies of prostate cancer cells and hepatocellular carcinoma treated with rapamycin and bortezomib, respectively [29,31]. We showed that 4E-BP1-mediated autophagy is independent of its role in protein translation (Fig. 3C and D), and it is the level of 4E-BP1 that closely associated with autophagy. Based on the facts that 4E-BP1 is also involved in mTORC1 complex, and mTOR regulates autophagy by dissociation from ULK1-Atg13-FIP200 complexes, we hypothesize that 4E-BP1 may play a role in stabilizing mTORC1-ULK1-Atg13-FIP200 complex. As a consequence of 4E-BP1 depletion, mTORC1 may release ULK1-Atg13-FIP200 so that favors the formation of autophagosomes. Research is ongoing in this regard.

In summary, our report revealed 4E-BP1 as a novel effector of PTL treatment along the path leading to autophagy. It is of clinical potential to reduce the cellular 4E-BP1 by the natural component

PTL. Nowadays, anticancer drugs act as inducers for autophagy in lymphoid malignancies have been under the intensive development in clinical trials [32,33]. Our study here may provide a novel strategy to enhance the drug potency or susceptibility of cancer therapeutics by combination with natural products or components.

Acknowledgments

The authors would like to thank Dr. Yue. Chen (Nankai University, China) for kindly providing parthenolide and Dr. Quan. Chen (Nankai University, China) for providing reagents and MEF cells. We also like to thank Dr. Qing. Zhong (University of California, Berkeley, USA) for providing the pGFP-LC3 plasmid.

This work was supported by grants from the Natural Science Foundation of China (81171556 and 31370862 to Y.C.), and the Ministry of Science and Technology of China (2012CB917204 to Y.C.); this work is also under the support of Program of Introducing Talents of Discipline to Universities (B08011) from the Ministry of Education of China.

References

[1] D.W. Knight, Feverfew: chemistry and biological activity, Nat. Prod. Rep. 12 (1995) 271–276.
[2] J.H. Kim, L. Liu, S.O. Lee, et al., Susceptibility of cholangiocarcinoma cells to parthenolide-induced apoptosis, Cancer Res. 65 (2005) 6312–6320.
[3] M.L. Guzman, R.M. Rossi, L. Karnischky, et al., The sesquiterpene lactone parthenolide induces apoptosis of human acute myelogenous leukemia stem and progenitor cells, Blood 105 (2005) 4163–4169.
[4] J. Wen, K.R. You, S.Y. Lee, et al., Oxidative stress-mediated apoptosis. The anticancer effect of the sesquiterpene lactone parthenolide, J. Biol. Chem. 277 (2002) 38954–38964.
[5] S. Zhang, C.N. Ong, H.M. Shen, Involvement of proapoptotic Bcl-2 family members in parthenolide-induced mitochondrial dysfunction and apoptosis, Cancer Lett. 211 (2004) 175–188.
[6] A.J. Garcia-Pineres, V. Castro, G. Mora, et al., Cysteine 38 in p65/NF-kappaB plays a crucial role in DNA binding inhibition by sesquiterpene lactones, J. Biol. Chem. 276 (2001) 39713–39720.
[7] M.T. Yip-Schneider, H. Nakshatri, C.J. Sweeney, et al., Parthenolide and sulindac cooperate to mediate growth suppression and inhibit the nuclear factor-kappa B pathway in pancreatic carcinoma cells, Mol. Cancer Ther. 4 (2005) 587–594.
[8] Z. Yang, D.J. Klionsky, An overview of the molecular mechanism of autophagy, Curr. Top. Microbiol. Immunol. 335 (2009) 1–32.
[9] G. Marino, M. Niso-Santano, E.H. Baehrecke, et al., Self-consumption: the interplay of autophagy and apoptosis, Nat. Rev. Mol. Cell Biol. 15 (2014) 81–94.
[10] L. Dubois, M.G. Magagnin, A.H. Cleven, et al., Inhibition of 4E-BP1 sensitizes U87 glioblastoma xenograft tumors to irradiation by decreasing hypoxia tolerance, Int. J. Radiat. Oncol. Biol. Phys. 73 (2009) 1219–1227.
[11] A.J. Steele, D.T. Jones, K. Ganeshaguru, et al., The sesquiterpene lactone parthenolide induces selective apoptosis of B-chronic lymphocytic leukemia cells in vitro, Leukemia 20 (2006) 1073–1079.
[12] T. Schmelzle, M.N. Hall, TOR, a central controller of cell growth, Cell 103 (2000) 253–262.
[13] C. Hu, S. Pang, X. Kong, et al., Molecular cloning and tissue distribution of PHAS-I, an intracellular target for insulin and growth factors, Proc. Natl. Acad. Sci. U.S.A. 91 (1994) 3730–3734.
[14] A. Haghighat, S. Mader, A. Pause, et al., Repression of cap-dependent translation by 4E-binding protein 1: competition with p220 for binding to eukaryotic initiation factor-4E, EMBO J. 14 (1995) 5701–5709.
[15] N. Hay, N. Sonenberg, Upstream and downstream of mTOR, Genes Dev. 18 (2004) 1926–1945.
[16] I. Mothe-Satney, D. Yang, P. Fadden, et al., Multiple mechanisms control phosphorylation of PHAS-I in five (S/T)P sites that govern translational repression, Mol. Cell. Biol. 20 (2000) 3558–3567.
[17] S. Mader, H. Lee, A. Pause, et al., The translation initiation factor eIF-4E binds to a common motif shared by the translation factor eIF-4 gamma and the translational repressors 4E-binding proteins, Mol. Cell. Biol. 15 (1995) 4990–4997.
[18] S.S. Schalm, D.C. Fingar, D.M. Sabatini, et al., TOS motif-mediated raptor binding regulates 4E-BP1 multisite phosphorylation and function, Curr. Biol. 13 (2003) 797–806.
[19] S. Zhang, C.N. Ong, H.M. Shen, Critical roles of intracellular thiols and calcium in parthenolide-induced apoptosis in human colorectal cancer cells, Cancer Lett. 208 (2004) 143–153.
[20] M.B. Azad, Y. Chen, S.B. Gibson, Regulation of autophagy by reactive oxygen species (ROS): implications for cancer progression and treatment, Antioxid. Redox Signal. 11 (2009) 777–790.
[21] J.A. McCubrey, M.M. Lahair, R.A. Franklin, Reactive oxygen species-induced activation of the MAP kinase signaling pathways, Antioxid. Redox Signal. 8 (2006) 1775–1789.
[22] A. D'Anneo, D. Carlisi, M. Lauricella, et al., Parthenolide generates reactive oxygen species and autophagy in MDA-MB231 cells. A soluble parthenolide analogue inhibits tumour growth and metastasis in a xenograft model of breast cancer, Cell Death Dis. 4 (2013) e891.
[23] C. Lu, W. Wang, Y. Jia, et al., Inhibition of AMPK/autophagy potentiates parthenolide-induced apoptosis in human breast cancer cells, J. Cell. Biochem. 115 (2014) 1458–1466.
[24] J. Sun, C. Zhang, Y.L. Bao, et al., Parthenolide-induced apoptosis, autophagy and suppression of proliferation in HepG2 cells, Asian Pac. J. Cancer Prev. 15 (2014) 4897–4902.
[25] C.B. Lim, P.Y. Fu, N. Ky, et al., NF-kappaB p65 repression by the sesquiterpene lactone. Helenalin, contributes to the induction of autophagy cell death, BMC Complement. Altern. Med. 12 (2012) 93.
[26] T. Itoh, K. Ohguchi, Y. Nozawa, et al., Intracellular glutathione regulates sesquiterpene lactone-induced conversion of autophagy to apoptosis in human leukemia HL60 cells, Anticancer Res. 29 (2009) 1449–1457.
[27] K. Moreau, S. Luo, D.C. Rubinsztein, Cytoprotective roles for autophagy, Curr. Opin. Cell Biol. 22 (2010) 206–211.
[28] Y.J. Chen, W.P. Huang, Y.C. Yang, et al., Platonin induces autophagy-associated cell death in human leukemia cells, Autophagy 5 (2009) 173–183.
[29] H.C. Yu, D.R. Hou, C.Y. Liu, et al., Cancerous inhibitor of protein phosphatase 2A mediates bortezomib-induced autophagy in hepatocellular carcinoma independent of proteasome, PLoS One 8 (2013) e55705.
[30] C.Y. Lai, S.L. Pan, X.M. Yang, et al., Depletion of 4E-BP1 and regulation of autophagy lead to YXM110-induced anticancer effects, Carcinogenesis 34 (2013) 2050–2060.
[31] B.S. Balakumaran, A. Porrello, D.S. Hsu, et al., MYC activity mitigates response to rapamycin in prostate cancer through eukaryotic initiation factor 4E-binding protein 1-mediated inhibition of autophagy, Cancer Res. 69 (2009) 7803–7810.
[32] A. Ertmer, V. Huber, S. Gilch, et al., The anticancer drug imatinib induces cellular autophagy, Leukemia 21 (2007) 936–942.
[33] Available at: <http://www.druglib.com/trial/09/NCT00136409.html> (2014-10-31).